Effect of Head-Group Structure and Counterion Condensation on Phase Equilibria in Anionic Phospholipid–Water Systems Studied by ^2H, ^{23}Na, and ^{31}P NMR and X-ray Diffraction†

Göran Lindblom,*,‡ Leif Rilfors,‡ Jön B. Hauksson,‡ Ingvar Brentel,‡ Mats Sjölund,‡ and Björn Bergenståhl§
Department of Physical Chemistry, University of Umeå, S-901 87 Umeå, Sweden, and Institute of Surface Chemistry, P.O. Box 5607, S-114 86 Stockholm, Sweden

Received January 4, 1991; Revised Manuscript Received August 23, 1991

ABSTRACT: The phase equilibria, hydration, and sodium counterion association for the systems DOPA–^2H_2O, DOPS–^2H_2O, DOPG–^2H_2O, and DPG–^2H_2O were investigated with ^2H, ^{23}Na, and ^{31}P NMR and X-ray diffraction. The following one-phase regions were found in the DOPA–water system: a reversed hexagonal liquid-crystalline (H_{II}) phase up to about 35 wt % water and a lamellar liquid-crystalline (L_α) phase between about 55 and 98 wt % water. The area per DOPA molecule was 36–65 Å^2 in the H_{II} phase (10–40 wt % water) and 69 Å^2 in the L_α phase (60 wt % water). DOPS and DOPG with 10–98 wt % water, and DPG with 20–95 wt % water formed an L_α phase at temperatures between 25 and 55 °C. At temperatures above 55 °C, DPG with 20 and 30 wt % water formed a mixture of L_α, H_{II}, and cubic liquid-crystalline phases, the mole percent of lipid forming nonlamellar phases being smaller at 30 wt % water than at 20 wt % water. DPG with 10 wt % water probably formed a mixture of an L_α phase and at least one nonlamellar liquid-crystalline phase at 25 and 35 °C, and a pure H_{II} phase at 45 °C and higher temperatures. At water concentrations above about 50 wt % the ^{23}Na quadrupole splitting was *constant* for all four lipid–water systems studied, implying that the counterion association to the charged lipid aggregates did not change upon dilution. These experimental observations can be described with an ion condensation model but not with a simple equilibrium model. The fraction of counterions located close to the lipid–water interface was calculated to be >95%. The ^2H and ^{23}Na NMR quadrupole splittings of ^2H_2O and sodium counterions, respectively, indicate that the molecular order in the polar head-group region decreases for the L_α phase in the order DOPA ≈ DPG > DOPS > DOPG.

The electrostatic properties of biological membranes play an important role for several fundamental processes occurring in the cell, and the ionic distribution close to the membrane might be of great importance for the cell function. It was recently reported (Antonenko & Yaguzhinsky, 1990) that changes in the cation concentration near the bilayer surface affect the cation fluxes and selectivity. Evidence has also been obtained that protons in proton-pumping membranes move along or within the bilayer rather than exchange with the bulk solution. It has been proposed (Haines, 1983) that anionic lipid head-groups, which are always present in proton-pumping membranes, trap and conduct protons along the head-group domain.

Changes in the interfacial tension in monolayers of phospholipids can induce a large change in the interfacial Gibbs energy by altering either the potential or the pH at the interface. This remarkable property of lipid layers allows a coupling between surface movement, pH, and the potential. It has been proposed (Girault & Schiffrin, 1986) that charges on the phospholipids of a membrane can provide a driving force for cell and organelle motility, phagocytosis, and streaming effects. Some experimental evidence has been presented that the local interfacial tension depends on both the lipid composition and the state of the head-group charge (Girault & Schiffrin, 1984).

Since ion transport across membranes is central to bioenergetics, the cell membrane must have mechanical properties that can cope with the arising osmotic pressure effects. The capacity of various bacteria to deal with osmotic swelling has been subjected to a large number of investigations. Thus, for example, several bacteria respond to an increase in the salinity of the culture medium by increasing the proportion of anionic lipids in the membrane (Kanemasa et al., 1972; Komaratat & Kates, 1975; Ohno et al., 1979; Kogut & Russell, 1984; Miller, 1985; Christiansson et al., 1985). To understand the origin of the observed salinity-induced changes in biomembrane composition, it is important to study the effects of salinity and surface charge density on the material properties of lipid bilayers (Rand & Parsegian, 1989). The result of the application of an osmotic stress on a cell membrane will strongly depend on the material properties, like the elasticity, the area compressibility modulus, and the curvature modulus, of the bilayer. For instance, an increase in the surface charge density of the lipid bilayer could restrict the expansion of the bilayer under osmotic stress, which is in accordance with the observation of an increase in the amount of anionic lipids of several bacteria.

Anionic lipids are present in all biological membranes. Phosphatidylglycerol (PG)[1] and diphosphatidylglycerol (DPG) are the predominant anionic lipids of bacterial membranes. These two lipids together with phosphatidylserine (PS) are common in eukaryotic cell membranes. Phosphatidic acid (PA) is a minor component of cell membranes, but it is a key intermediate in the biosynthesis of other phosphoglycerides. Reusch (1990) observed that alkali metal ions influence the

† This work was supported by the Swedish Natural Science Research Council, the Knut and Alice Wallenberg Foundation, and the Carl Trygger Foundation.

‡ University of Umeå.
§ Institute of Surface Chemistry.

[1] Abbreviations: L_β, lamellar gel phase; L_α, lamellar liquid-crystalline phase; T_m, temperature for the L_β to L_α phase transition; H_{II}, reversed hexagonal liquid-crystalline phase; DO, dioleoyl; PA, phosphatidic acid; PG, phosphatidylglycerol; PS, phosphatidylserine; DPG, diphosphatidylglycerol; PC, phosphatidylcholine; PE, phosphatidylethanolamine; MGlcDG, monoglucosyldiacylglycerol; DGlcDG, diglucosyldiacylglycerol; CSA, chemical shift anisotropy; NMR, nuclear magnetic resonance.

0006-2960/91/0430-10938$02.50/0

PA-mediated Ca^{2+} transport in a unique way; monovalent cations were found to be essential for the transport, and the physiologically abundant Na^+ and K^+ ions induce a sharp increase in the transport at critical concentrations.

Certainly, armed with a detailed knowledge of the physicochemical properties of anionic membrane lipids, like headgroup hydration, counterion association, lipid aggregate structure, monolayer curvature, and the phase behavior, we will be in a good position to get a better understanding of biological processes where anionic lipids are involved. So far, comparatively little has been reported on the ionic lipids, and below we will briefly summarize the phase behavior of some anionic lipids.

Due to the net negative charge of anionic lipids at physiological pH values, the interaction with monovalent and divalent cations, and changes of the pH value in these lipid–water systems, will affect the phase equilibria. The unique behavior of many charged lipids to swell and form unilamellar vesicles in excess water has been reviewed by Hauser (1984). The temperature (T_m) for the transition between a lamellar gel (L_β) phase and a lamellar liquid-crystalline (L_α) phase is profoundly increased for PG and PS by addition of Ca^{2+} (Verkleij et al., 1974; Jacobson & Papahadjopoulos, 1975). This transition temperature is also increased for PG and PS when the pH is changed from neutral to acidic values (Verkleij et al., 1974; Jacobson & Papahadjopoulos, 1975; Mombers et al., 1977; Findlay & Barton, 1978; Van Dijck et al., 1978). When the pH is decreased, a monolayer of PS molecules is condensed (Demel et al., 1987), and the orientational order of the acyl chains in a PS bilayer is increased (De Kroon et al., 1990). In a theoretical and experimental work, Kaminoh et al. (1988) investigated the effect of surface ionization of dimyristoyl-PA on the L_β–L_α phase transition. It was found that, according to the theory, T_m decreased with increasing pH, apparently due to the change in ionization and the resulting increase in the electrostatic repulsion between the negatively charged lipid head-groups. A transition from an L_α to a reversed hexagonal (H_{II}) phase is induced by the addition of Ca^{2+}, Mg^{2+}, or Mn^{2+} to DPG and PA (Rand & Sengupta, 1972; Cullis et al., 1978; Van Venetië & Verkleij, 1981, Verkleij et al., 1982), by the addition of Na^+ to DPG (Seddon et al., 1983), and by the addition of Li^+ to PS (Cevc et al., 1985). The L_α–H_{II} phase transition also occurs for PS, PA, and DPG when the pH is decreased from a neutral to an acidic value (Hope & Cullis, 1980; Harlos & Eibl, 1981; Verkleij et al., 1982; Farren et al., 1983; Seddon et al., 1983; De Kroon et al., 1990). Changes in the concentration of cations and the pH can induce fusion of anionic lipid vesicles (Papahadjopoulos et al., 1977) and affect the composition in biological membranes (Op den Kamp et al., 1969, and references above).

The studies mentioned above were performed with lipid–water mixtures in which the water concentration was around 95 wt %. In this study, the phase equilibria and the counterion association of the sodium salts of DOPA, DOPS, DOPG, and DPG were investigated with X-ray diffraction and ^2H, ^{23}Na, and ^{31}P NMR at water concentrations ranging from 10 to 98 wt % ^2H_2O. DOPA behaves differently than the other three lipids; it forms an H_{II} phase up to about 35 wt % water. Above approximately 50 wt % water, the counterion concentration close to the lipid–water interface is *constant* and very high in all the anionic lipid–water systems studied.

Materials and Methods

Sample Preparation. Dioleoylphosphatidylcholine (DOPC) and the sodium salts of dioleoylphosphatidic acid (DOPA), dioleoylphosphatidylserine (DOPS), and dioleoylphosphatidylglycerol (DOPG) were obtained from Avanti Polar Lipids, Inc., Birmingham, AL. The purity was given as >99%. Thin-layer chromatography analysis of the lipids showed about 1% of contamination in DOPG, and no further purification was done. The sodium salt of bovine heart DPG and *n*-dodecane were purchased from Sigma Chemical Co., St. Louis, MO, and deuterium oxide was obtained from Ciba Geigy. The purity of DPG was >99%, as judged by thin-layer chromatography.

The samples were prepared in small test tubes from lipids dried to constant weight in vacuum. Pure or buffered deuterium oxide was added, and the tubes were immediately sealed. The samples were mixed by centrifugation and subjected to several freeze–thaw cycles. NMR spectra were recorded repeatedly from all samples during a period of 2–3 months. DOPA was degraded when heated to 45–55 °C, and samples that had been heated to these temperatures were discarded.

NMR Spectroscopy. Experimental work with phase diagrams is usually very time consuming, in particular using classical methods, and the need for more efficient methods led to the development of, above all, NMR techniques for such determinations (Ulmius et al., 1977). These convenient methods, based on ^2H and ^{31}P NMR, have been frequently utilized by us (Brentel et al., 1985, 1987; Arvidson et al., 1985; Eriksson et al., 1985; Lindblom et al., 1986, 1988; Sjölund et al., 1987, 1989), and these NMR methods have been used also here.

^{31}P NMR spectra were obtained with a Bruker ACP-250 Fourier transform spectrometer at 101.3 MHz. A phase-cycled Hahn echo sequence (Rance & Byrd, 1983) was used. Inverse gated high-power proton decoupling was applied during the aquisition. The echo time was 50 μs, the spectral width 100 kHz, the pulse length 10 μs (90°), and the relaxation delay 1 s. For a typical spectrum, 3000–5000 scans were accumulated, and an exponential multiplication corresponding to 20 Hz line broadening was applied before the Fourier transformation. The free induction decay (FID) was left-shifted prior to the exponential multiplication until the first point of the FID represented the maximum of the echo.

^2H and ^{23}Na NMR spectra were recorded on a Bruker ACP-250 spectrometer at 38.4 and 66.2 MHz, respectively. ^2H NMR spectra were recorded using the quadrupole echo sequence (Davis et al., 1976) with a 90° pulse width of 20 μs, a spectral width of 100 kHz, and an interpulse spacing of 50 μs. The delay time between the pulse sequences was 1.0 s. Typically 1000 transients were collected. ^{23}Na NMR spectra were recorded using a simple one pulse sequence with a 60° pulse width of 15 μs, a spectral width of 100 kHz, and a pulse repetition rate of 10 s^{-1}. Typically 50 000–100 000 transients were required for an adequate signal-to-noise ratio. The FID was left-shifted prior to the Fourier transformation in order to remove the broad signal resulting from the glass in the test tube. The ^2H quadrupole splittings were obtained from the peak separation, and the ^{23}Na quadrupole splittings were obtained from the distance between the central line and one of the adjacent lines. The samples were thermally equilibrated for about 1 h before initiation of NMR measurements.

X-ray Investigations. X-ray diffraction was applied to identify the structures, and to estimate the structure parameters, of the liquid-crystalline phases in the DOPA–water system. The interpretations follow Fontell et al. (1968). X-ray diffraction was recorded with a low-angle Kiessig camera equipped with a position-sensitive electronic detector (PSD 100, Tennelec Inc., Oak Ridge, TN). The X-ray source was

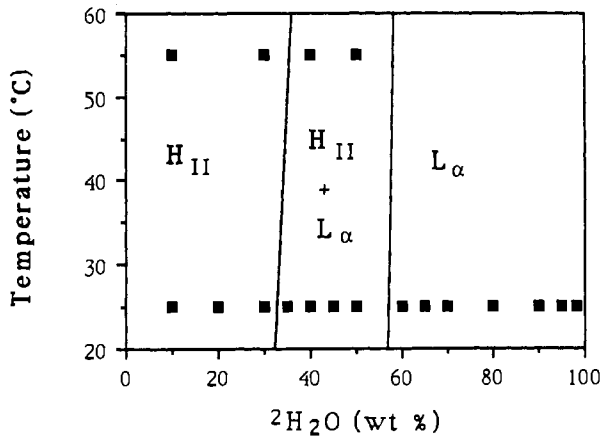

FIGURE 1: Tentative phase diagram for the system DOPA–^2H_2O. The phase equilibria were deduced by ^{31}P NMR and X-ray diffraction. The reversed hexagonal and the lamellar liquid-crystalline phases are denoted by H_{II} and L_α, respectively.

Ni-filtered Cu Kα radiation. Measurements were made in the range 0.12–1.7°. About 1 min exposures were required to obtain good diffraction patterns. The detector was repeatedly calibrated with crystalline sodium octanoate (repeat distance 23 Å). The samples were contained in freshly prepared flame-sealed glass capillaries. The Bragg distance from the first diffraction line was used to calculate the repeat distances, the thickness of the water layer in the L_α phases, the diameter of the water cylinder in the H_{II} phases, and the area per lipid molecule.

Results

DOPA–^2H_2O Phase Equilibria. ^{31}P NMR measurements were performed in the temperature range 25–75 °C at water concentrations between 10 and 98 wt %. Figure 1 shows a tentative phase diagram for the system DOPA–^2H_2O. Samples with 10, 20, and 30 wt % ^2H_2O gave ^{31}P NMR spectra exhibiting a low-field peak and a high-field shoulder (Figure 2A); such spectra are characteristic of a hexagonal phase (McLaughlin et al., 1975). The phase is most probably of the reversed type (H_{II}) since the water contents are rather low and since this hexagonal phase is formed at *lower* water contents than the L_α phase (see below). The chemical shift anisotropy (CSA) was +18 ppm. Low-angle X-ray diffraction investigations of samples with 10, 20, and 30 wt % ^2H_2O gave diffractograms with a pattern characteristic of a hexagonal phase ($1:\sqrt{3}:\sqrt{4}$). The X-ray results are shown in Figure 3. The repeat distance, the diameter of the water cylinder, and the area per lipid head-group in the H_{II} phase increase with increasing water content. Studies of the X-ray samples with polarized light microscopy showed a fan-like texture, further supporting the interpretation that they formed a hexagonal phase (Rosevear, 1954, 1968).

DOPA–^2H_2O mixtures with 35, 40, 45, 50, and 54 wt % water gave ^{31}P NMR spectra with a superposition of line shapes typical for an H_{II} phase and an L_α phase (low-field shoulder and high-field peak) (Figure 2B). The CSA for the L_α phase was −35 ppm. In the sample with 35 wt % water, 88 and 12 mol % of the lipid was in the H_{II} and L_α phases, respectively; with 40 wt % water, 65 and 35 mol % of the lipid was in the H_{II} and the L_α phase, respectively, while with 50 wt % water the corresponding values were 27 and 73 mol %. All values were obtained by simulating the experimental ^{31}P NMR spectra recorded at 25 °C. An increased temperature displaced the equilibria in these two-phase samples toward the H_{II} phase. For example, about 80 mol % DOPA in the sample with 40 wt % ^2H_2O formed an H_{II} phase at 55 °C. The X-ray

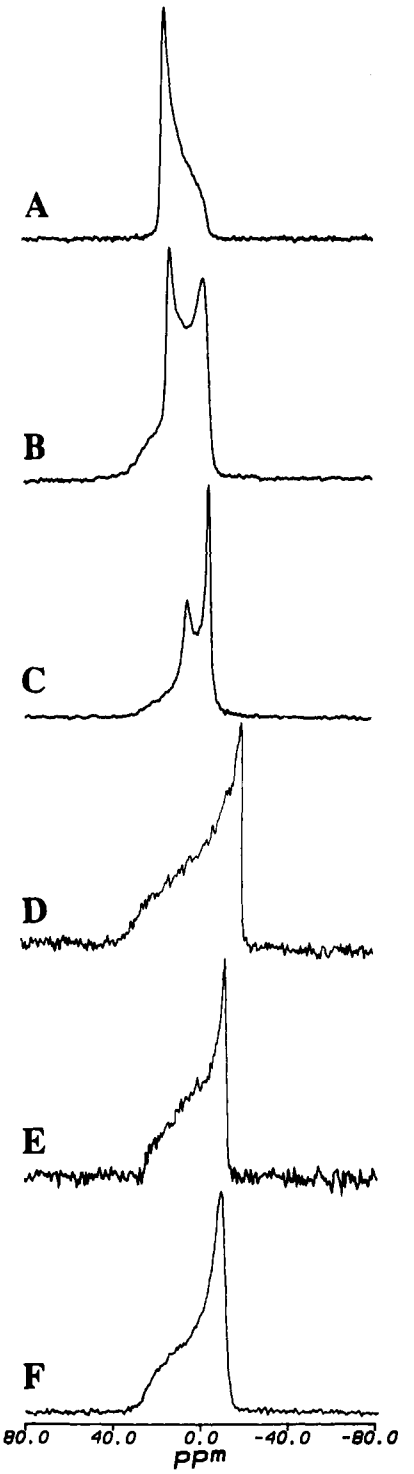

FIGURE 2: ^{31}P NMR spectra recorded at 101.3 MHz from samples composed of ^2H_2O and different anionic phospholipids: (A) DOPA with 20 wt % ^2H_2O at 25 °C; (B) DOPA with 45 wt % ^2H_2O at 25 °C; (C) DOPA with 95 wt % ^2H_2O at 25 °C; (D) DOPS with 10 wt % ^2H_2O at 25 °C; (E) same as panel D at 55 °C; (F) DOPG with 50 wt % ^2H_2O at 25 °C.

diffractogram for a DOPA sample with 40 wt % water followed the hexagonal pattern ($1:\sqrt{3}:\sqrt{4}$), but a coexisting lamellar phase could not be excluded. Since ^{31}P NMR proved the presence of both the phases in this sample (see above), the Bragg distance was used to calculate the structure parameters for both the phases (Figure 3). The X-ray diffractogram from the DOPA sample with 50 wt % water showed only a pattern characteristic of a lamellar phase (1:2:3:4), while ^{31}P NMR showed that the L_α phase dominates at this water concen-

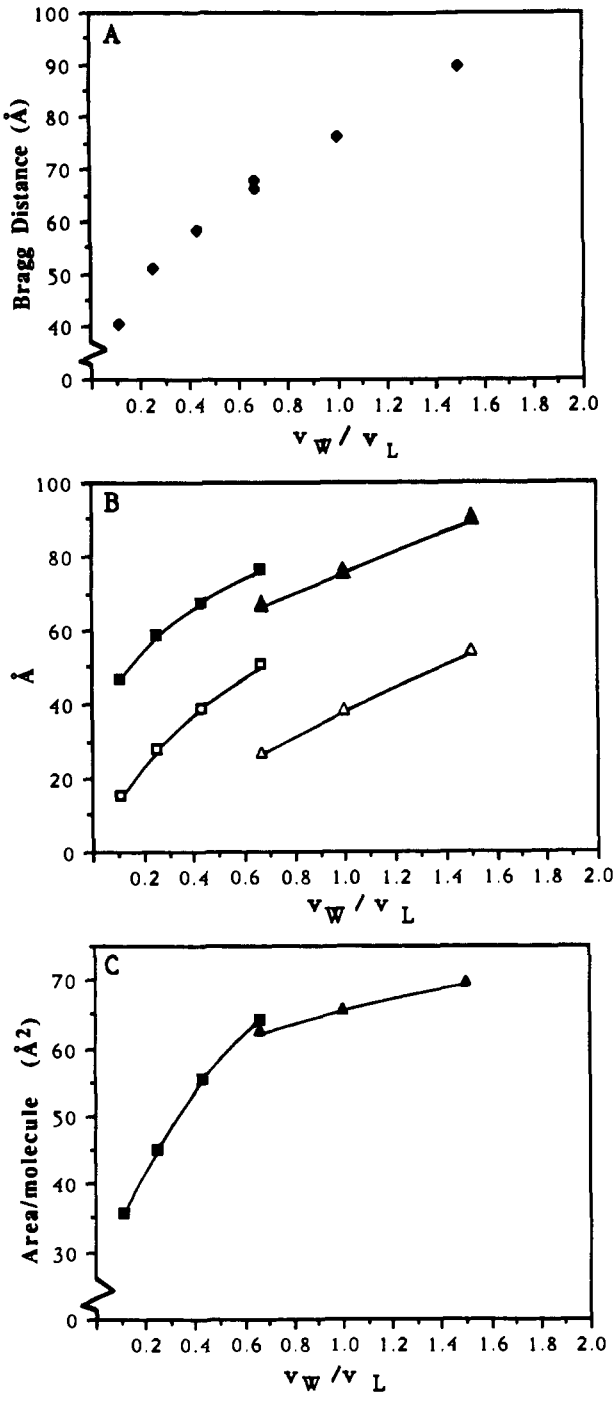

FIGURE 3: X-ray diffraction results for DOPA. (A) Bragg distances in angstroms versus the volume ratio for water and lipid (v_W/v_L). (B) The repeat distance (■) and the water cylinder diameter (□) for the H_{II} phase and the repeat distance (▲) and the water layer thickness (△) for the L_α phase vs v_W/v_L. (C) The area per lipid molecule in Å² vs v_W/v_L for the H_{II} phase (■) and the L_α phase (▲).

tration. Consequently, the X-ray results were used to calculate the structure parameters for only the L_α phase (Figure 3). The bilayer thickness was calculated to be 40 and 38 Å in DOPA–water mixtures with 40 and 50 wt % water, respectively.

^{31}P NMR showed that DOPA samples containing 60–98 wt % ^2H_2O form an L_α phase (Figure 1). A sample with 60 wt % ^2H_2O gave an X-ray diffractogram with a pattern characteristic of a lamellar phase (1:2:3:4) (Figure 3). ^{31}P NMR spectra recorded from fresh samples often exhibited a narrow symmetrical signal together with the spectral component derived from the L_α phase (Figure 2C). The narrow symmetrical signal disappeared when the samples were subjected to freeze–thaw cycles. The origin of the narrow signal is probably vesicles that form spontaneously during the sample preparation (Hauser, 1989). The low-field shoulder in the ^{31}P NMR spectra recorded from samples with 95 wt % ^2H_2O was reduced considerably with time; the spectrum shown in Figure 5B was recorded about 3 weeks later than the spectrum shown in Figure 2C.

The effect of adding buffer, NaCl, and *n*-dodecane was investigated with a water concentration (54 wt %) that gave a mixture of L_α and H_{II} phases with pure ^2H_2O (Figure 1). *n*-Dodecane has previously been shown to have a drastic effect on the phase equilibria in PC–water systems (Sjölund et al., 1987, 1989; Lindblom et al., 1988). When 2 mol of *n*-dodecane per mol of DOPA was added to a sample with water buffered to p^{2}H 7.2 [50 mM Tris–acetic acid and 2 mM EDTA; for pK_a values of DOPA, see Hauser (1989)], an isotropic phase, together with a small fraction of L_α and H_{II} phases, was formed. The presence of *n*-dodecane in a sample with buffer and 100 mM NaCl induced the formation of a pure isotropic phase. In this case, the isotropic phase is probably not vesicles; instead it might be a cubic phase.

DOPS–^2H_2O Phase Equilibria. The phase equilibria were studied at water concentrations between 10 and 98 wt % ^2H_2O. ^{31}P NMR spectra were recorded at 25 °C for all samples and at 55 °C for the sample with 10 wt % water. All spectra show only a line shape characteristic of an L_α phase (Figure 2D). The CSA for DOPS at 25 °C was between −52 and −55 ppm at all water contents. However, the CSA was reduced to −40 ppm at 55 °C in the sample with 10 wt % ^2H_2O (Figure 2E). ^{31}P NMR spectra recorded from fresh DOPS–^2H_2O samples containing 70 wt %, or more, water showed a narrow symmetrical signal together with the spectral component from the L_α phase; the narrow signal disappeared after a freeze–thaw cycle (cf. DOPA). The low-field shoulder of the ^{31}P NMR spectra from the sample with 98 wt % water was reduced with time.

DOPG–^2H_2O Phase Equilibria. DOPG behaves in the same way as DOPS and forms an L_α phase at water contents between 10 and 98 wt % ^2H_2O in the temperature interval 25–55 °C (Figure 2F); the CSA for DOPG was between −32 and −34 ppm. In contrast to DOPA and DOPS, an isotropic phase was not formed in fresh samples.

The effect of adding buffer (p^{2}H 7.2; see above), 100 mM NaCl, and *n*-dodecane was investigated with DOPG in the same way as with DOPA. DOPG–^2H_2O mixtures with 54 wt % water still formed an L_α phase between 25 and 55 °C in the presence of buffer, or buffer and NaCl. When 2 mol of *n*-dodecane per mol of DOPG was added as well, an H_{II} phase, with a small fraction of an L_α phase, was formed at 25 °C, and a pure H_{II} phase was formed at 55 °C. DOPG was also used to investigate the ability of an anionic membrane lipid to affect the phase equilibria of a DOPC–*n*-dodecane–^2H_2O (1:2:46 mol/mol) system forming an H_{II} phase (Sjölund et al., 1987, 1989; Lindblom et al., 1988). Incorporation of 10, 20, or 50 mol % DOPG in this system had no effect on the phase equilibria. Unexpectedly, a sample with DOPG–*n*-dodecane–^2H_2O (1:2:46 mol/mol) also formed an H_{II} phase.

DPG–^2H_2O Phase Equilibria. ^{31}P NMR measurements were performed in the temperature range 25–75 °C at water concentrations between 10 and 95 wt %. Representative spectra are shown in Figure 4. At 10 wt % water, and at 25 and 35 °C, both ^2H and ^{31}P NMR show spectra that cannot easily be given a straightforward interpretation. Most probably the line shapes obtained originate from either a nonuniaxial

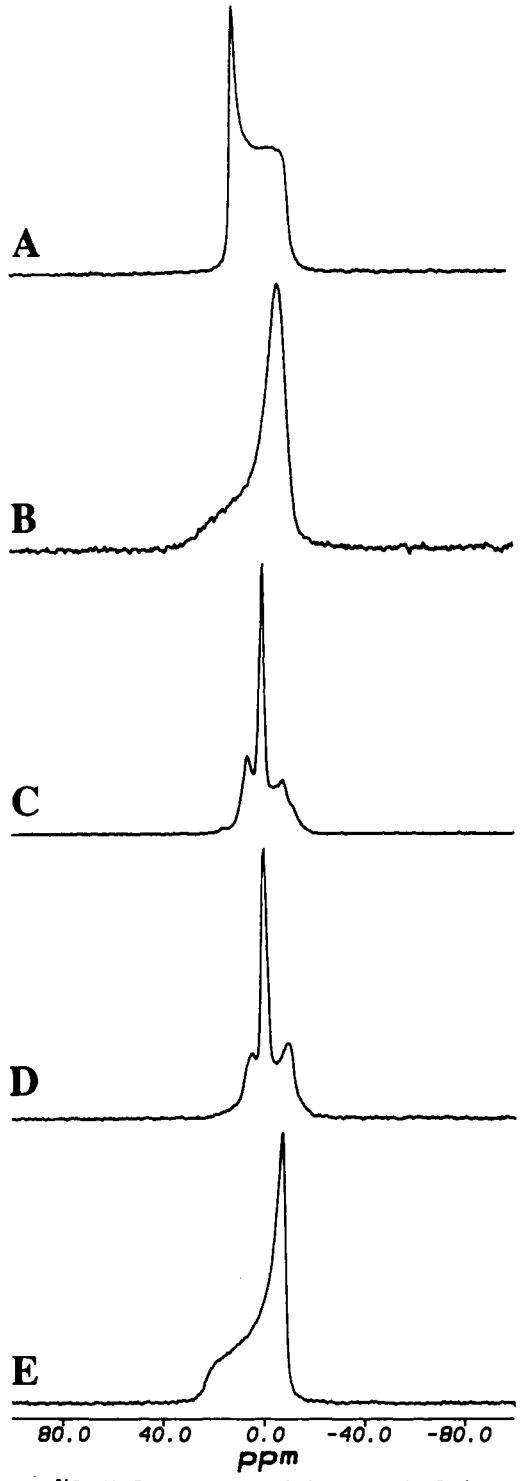

FIGURE 4: ^{31}P NMR spectra recorded at 101.3 MHz from samples containing DPG and ^2H_2O at various water contents and temperatures. (A) 10 wt % ^2H_2O at 65 °C; (B) 20 wt % ^2H_2O at 25 °C; (C) 20 wt % ^2H_2O at 65 °C; (D) 30 wt % ^2H_2O at 65 °C; and (E) 75 wt % ^2H_2O at 25 °C.

phase structure or from a mixture of phases including at least one nonlamellar phase. At temperatures from 45 to 75 °C, this sample gave ^{31}P NMR spectra with a low-field peak and a high-field shoulder (Figure 4A) indicative of a hexagonal phase (most probably an H_{II} phase; see above). The CSA was between +16 and +17 ppm. The intensity of the shoulder was, however, larger than expected for a randomly oriented powder sample, possibly due to either partial alignment of the cylinders along the axis of the applied magnetic field or possibly the presence of a nonuniaxial phase structure. Between 20 and 95 wt % water, an L_α phase was formed up to approximately 55 °C [Figure 4B,E; see also Rilfors et al. (1986)]; the CSA was between −29 and −31 ppm. A very small amount of nonlamellar phases was seen at 55 °C with 20 and 30 wt % water. Raising the temperature of these samples further gave a mixture of three phases, L_α, H_{II}, and a cubic phase. For example, at 65 °C the sample with 20 wt % water had 24, 38, and 38 mol % DPG in the L_α, H_{II}, and cubic phases, respectively (Figure 4C), while at 75 °C the corresponding values were 14, 72, and 14 mol %. When the water content was raised to 30 wt %, the phase equilibria were shifted toward the L_α or the cubic phase; at 65 °C, 44, 22, and 34 mol % DPG was in the L_α, H_{II}, and cubic phases, respectively (Figure 4D), while the corresponding values at 75 °C were 15, 63, and 22 mol %. These values were obtained by simulating the experimental spectra until virtually perfect fits were obtained.

Lipid Hydration. The molecular order of water in L_α and H_{II} phases is very conveniently determined from an investigation of ^2H NMR spectra of ^2H_2O (Persson et al., 1974; Ulmius et al., 1977; Brentel et al., 1985). Usually, an anisotropic liquid-crystalline phase gives a spectrum with a quadrupolar splitting. However, at high water contents the splittings might not be resolved due to chemical exchange between randomly oriented microcrystallites (Lindblom et al., 1976a).

A superposition of a narrow peak of low intensity and a quadrupolar splitting was obtained from DOPA with 90 and 95 wt % ^2H_2O (Figure 5A). DOPS with 98 wt % ^2H_2O and DPG with 75 wt % ^2H_2O gave ^2H NMR spectra with a splitting of 3 and 195 Hz, respectively, and without a narrow central peak. In contrast, ^2H NMR spectra recorded from DOPG did not show any resolved splittings at water contents above 50 wt %. The water deuteron splitting as a function of the water content for the DOPA–water system is shown in Figure 6. The same type of plots were made for the three other lipid–water systems (see Supplementary Material). The L_α phase formed at high water contents must be treated carefully. To observe the quadrupolar splittings, the samples must not be shaken; otherwise, just a single narrow peak is obtained.

Two splittings (one well resolved and one unresolved or poorly resolved) were obtained in ^2H NMR spectra recorded from DOPA with 10 wt % ^2H_2O, DOPS with 10 and 30 wt % ^2H_2O, DOPG with 10, 20, and 30 wt % ^2H_2O and DPG with 10 wt % ^2H_2O. The larger splitting for DOPA, DOPS, and DOPG probably derives from the heavy water and the smaller splitting from an $-O^2H$ group on the lipid. The origin of the two splittings for DPG is uncertain since ^{31}P NMR indicates the presence of more than one phase.

Contrary to what is generally expected, the water deuteron splitting for a sample composed of DOPA and 90 wt % ^2H_2O increased slightly (4 Hz) when the temperature was increased from 20 to 35 °C.

Sodium Counterion Association. Of the four anionic lipids investigated in this work, some DOPA–^2H_2O samples containing 90 and 95 wt % water formed an L_α phase that slowly became completely macroscopically aligned. Such samples gave ^{23}Na NMR spectra in which all the spectral intensity is present in a narrow central peak and two satellites (Figure 5C). The relationship between the peak intensities is 3:4:2.6, which is near the theoretically expected relationship (3:4:3) for a completely oriented liquid-crystalline phase. The bilayers in the L_α phase are oriented parallel with the magnetic field, since the value of the ^2H and the ^{23}Na NMR quadrupole splittings of the oriented and nonoriented (see below) samples are the

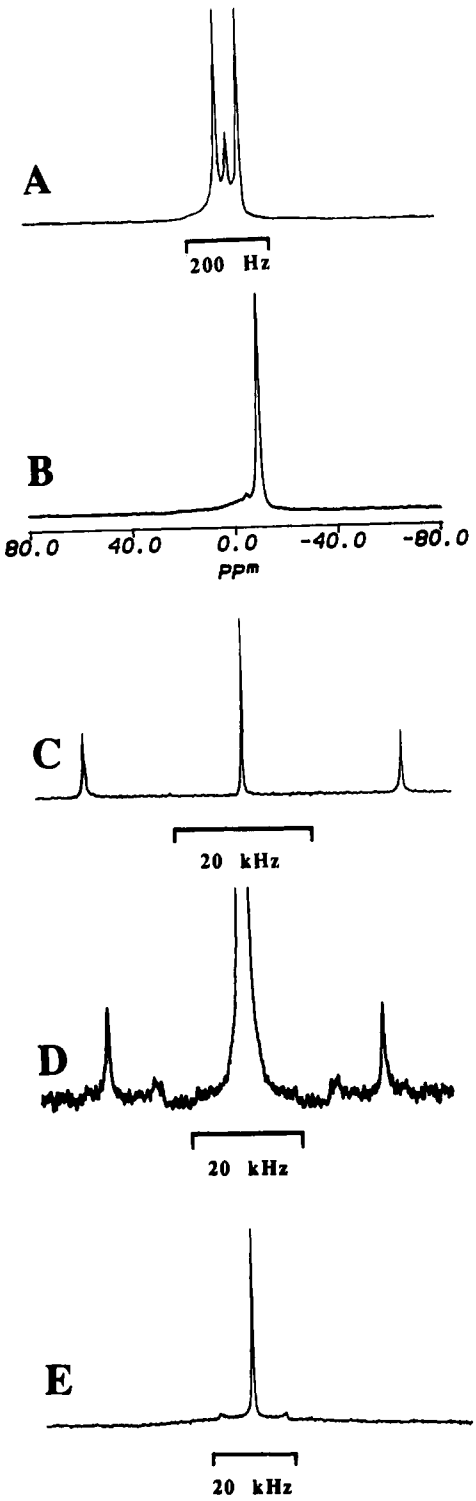

FIGURE 5: (A–C) NMR spectra from a macroscopically aligned L_α phase composed of the disodium salt of DOPA and 95 wt % ^2H_2O at 25 °C: (A) ^2H NMR; (B) ^{31}P NMR; (C) ^{23}Na NMR; (D) ^{23}Na NMR spectrum at 25 °C of a sample composed of DOPA and 45 wt % ^2H_2O, forming a mixture of H_{II} and L_α phases; and (E) ^{23}Na NMR "powder" spectrum of a sample of the sodium salt of DOPG and 30 wt % ^2H_2O.

same, i.e., the director of the oriented sample is perpendicular to the magnetic field (Lindblom, 1972). A ^{31}P NMR spectrum recorded from an oriented sample exhibits a considerably reduced low-field shoulder (Figure 5B). ^{23}Na NMR spectra recorded from the other samples of DOPA, and from all except one sample of DOPS, DOPG, and DPG, exhibited a narrow central peak together with satellite peaks of low intensity (Figure 5E), at all water contents investigated. This spectral

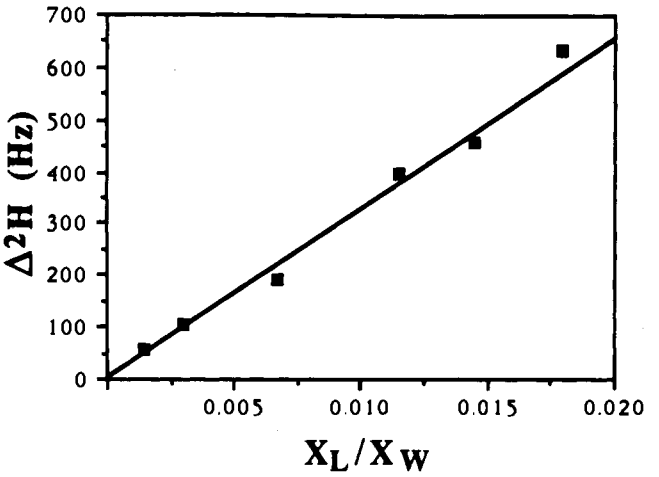

FIGURE 6: Water ^2H NMR quadrupole splitting as a function of the ratio between the mole fractions of lipid (X_L) and water (X_W) in the L_α phase of the DOPA–water system at 25 °C.

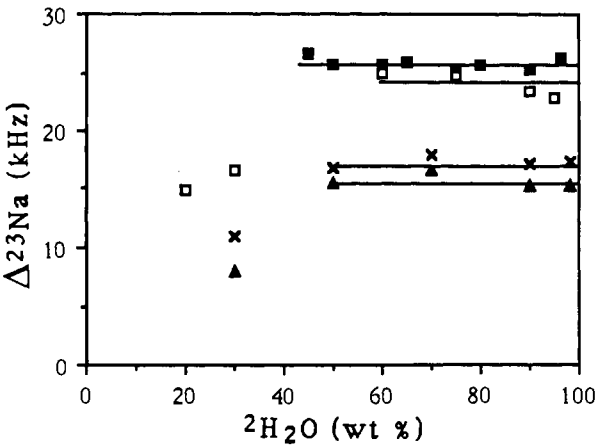

FIGURE 7: ^{23}Na NMR quadrupole splittings for the DOPA–^2H_2O (■), DOPS–^2H_2O (x), DOPG–^2H_2O (▲), and DPG–^2H_2O (□) systems as a function of the water content at 25 °C.

Table I: Slopes ($n|\chi S|$) of the Lines for the ^2H NMR Quadrupole Splittings (Δ^2H) versus the Ratio of the Mole Fractions of Lipid and Water (X_L/X_W) at High Water Concentrations, Where a Two-Site Model Is Applicable (cf. Figure 6), and the ^{23}Na NMR Quadrupole Splittings ($\Delta^{23}Na$) at High Water Concentrations, Where These Have Reached Constant Values (cf. Figure 7)

lipid	$n\|\chi S\|$ (kHz)	$\Delta^{23}Na$ (kHz)
DOPA	33.8	25.6
DPG	34.9	24.9
DOPS	21.2	17.3
DOPG	15.5	15.2

shape is characteristic of randomly oriented microcrystallites in a liquid-crystalline phase (so-called "powder pattern"). A sample of DPG with 10 wt % water gave a ^{23}Na NMR spectrum with only a narrow central peak; this kind of spectrum is obtained from powder samples with rapid exchange of sodium ions between the randomly oriented microcrystallites. The disappearence of the satellite peaks might also be due to line broadening, which makes it difficult to detect these spectral components.

Figure 7 shows ^{23}Na splittings obtained from the DOPA–^2H_2O, DOPS–^2H_2O, DOPG–^2H_2O, and DPG–^2H_2O systems as a function of the water content. At water contents above 50 wt %, the ^{23}Na splittings are approximately constant (Table I). For DPG, DOPS, and DOPG, the ^{23}Na splittings decrease when the water content is decreased below 50 wt % (Figure 7). A DOPA–^2H_2O sample with 45 wt % water, forming a

mixture of L_α and H_{II} phases (Figure 1), gave a ^{23}Na NMR spectrum with two pairs of satellite peaks (Figure 5D); the ^{23}Na splittings are 26.8 and 16.2 kHz for the L_α and H_{II} phase, respectively.

In resemblance with the ^2H NMR splittings, the ^{23}Na NMR splittings for DOPA with 95 wt % ^2H_2O increased (about 2 kHz) when the temperature was raised from 25 to 65 °C.

Discussion

Biological membranes contain numerous anionic and polar groups, many of which are located in the polar head-groups of the various membrane lipids. In the introduction, a number of examples were mentioned where electrostatic interactions and charged lipids may play a crucial role in biological processes. In particular, the presence of charges on a membrane surface can lead to an accumulation of ions and other charged species near the surface. To get a better understanding of such processes, and how charged lipids might be involved in membrane functions, we have investigated the physicochemical properties of some of the most common anionic membrane lipids.

In general, membrane lipid–water systems exhibit a rich polymorphism. Therefore, a natural starting point in this investigation of DOPA, DOPS, DOPG, and DPG was the determination of at least part of the lipid–water phase diagrams (Figures 1, 2, and 4).

Phase Equilibria. A qualitative understanding of the phase behavior of lipid–water systems can be arrived at by simple, but most useful, theoretical models. The phase structures may be controlled by the spontaneous radius of curvature of the lipid monolayer. Lipid compositions that can adopt negative values of this curvature (i.e., lipid monolayers curved around water regions) form stable reversed liquid-crystalline phases (Tate et al., 1991). The ability of a lipid monolayer to adopt negative radii of curvature is determined in part by the ability of the head-groups to be packed closely together: the area per lipid molecule is smaller at the head-group than in the hydrocarbon chain region for a monolayer with negative curvature. One would think that a lipid with a charged head-group would be less prone to adopt such a closely packed configuration due to electrostatic repulsion between the head-groups. Hence, these lipids should have a smaller tendency to adopt reversed phase structures than uncharged lipids with otherwise similar chemical structures. Steric interactions between head-groups must also affect their ability to pack closely together. Therefore, we might expect lipids with bulkier head-groups to be less prone to form reversed phases.

To account for these tendencies, Israelachvili and co-workers (1980) defined a packing parameter in terms of the hydrocarbon chain volume, the area per molecule at the lipid–water interface, and the length of the hydrocarbon chains. However, the value of each of these factors depends upon the nature of the phase in which the lipid is found, and upon the temperature and ambient conditions. For instance, the value of the packing parameter for DOPE changes significantly over a small temperature range (Tilcock & Cullis, 1982; Kirk & Gruner, 1985). Therefore, while this formalism is of great heuristic value, it is of limited utility in making explicit predictions about the temperature and composition dependence of lipid phase behavior. For explicit calculations of the relative stability of lamellar and reversed phases, a phenomenological model of material physics introduced by Helfrich (1973) has great advantages, although the molecular details are concealed. In this model, the lipid aggregate stability is dominated by an elastic free energy of curvature, and a concept related to the packing parameter, namely the so-called spontaneous curvature of the lipid monolayer, is utilized (Helfrich, 1973; Gruner, 1985; Hyde, 1989; Lindblom & Rilfors, 1989, 1990).

Gruner and co-workers have shown that the energy of curvature plays a dominant role in the formation of H_{II} phases for some zwitterionic phospholipids. For a phospholipid monolayer to form a cylinder there will also be a nonzero packing energy (Gruner, 1985). In particular, the hydrocarbon chains of the phospholipid molecules must stretch to fill the interstitial regions between the cylindrical aggregates building up the H_{II} phase. The smaller the radius of the water cylinder, the smaller are the hydrophobic interstices and the easier it is for the lipid acyl chains to elongate to fill the volume (Gruner, 1985; Tate & Gruner, 1987; Lindblom & Rilfors, 1990; Tate et al., 1991).

The phase behavior of the four anionic phospholipids investigated here can be given a reasonable explanation according to these simple theories. As can be inferred from Figure 1, an H_{II} phase is formed for the DOPA–water system up to a water content of about 35 wt %, and an L_α phase can swell up to a water concentration of at least 95 wt %. The space occupied by the head-group of an isolated DOPA molecule (i.e., without a hydration shell) is less than that occupied by DOPC, DOPS, DOPG, and DPG. When a large fraction of DOPA molecules is neutralized by association of counterions, the head-groups can probably be packed quite closely together. Therefore, the lipid monolayer should be more able to adopt a negative curvature, leading to the formation of an H_{II} phase. This tendency will increase with the degree of neutralization. Charge neutralization of lipids with acidic head-groups can often be achieved by reducing the pH value: DOPA, DOPS, and DPG form an H_{II} phase at acidic pH values (see the introduction). With increasing water concentration in the DOPA–water system, the interstitial regions between the growing lipid–water cylinders, building up the H_{II} phase, will increase. The creation of such void volumes is energetically unfavorable and will eventually lead to a transition to an L_α phase at a certain water content (Figure 1). Note that, since the H_{II} phase is in equilibrium with an L_α phase and not with excess water, all the water in the H_{II} phase has to be incorporated into the water cyclinders. When the water concentration is further increased, the L_α phase swells to very large distances between the charged bilayers, due to the long-reaching Coulombic forces. It is well known that even a small increase in the surface charge density may drastically increase the ability to take up water in a lamellar phase (Gulik-Krzywicki et al., 1969; Brentel et al., 1987). The thickness of the water layer at 98 wt % water for the DOPA system was estimated by an approximate calculation to be almost 2000 Å.

DPG forms an L_α phase at 25 °C with water concentrations between 20 and 95 wt % (Figure 4). The DPG molecule contains four acyl chains, and at neutral pH values it has one negative charge per two acyl chains. The presence of a hydroxylic group on the DPG head-group results in a further increase in the interfacial surface area per acyl chain and thus to a decrease in the surface charge density, as compared to DOPA. This may lead to a slightly less effective screening of the lipid head-group charges by counterion association. In all, the molecular shape of DPG at ambient temperature is probably more cylindrical-like, giving rise to the formation of bilayers. However, DPG is able to form H_{II} and cubic phases at low water contents and temperatures above 45–50 °C (Figure 4; Rand & Sengupta, 1972). Cubic phases are often located between L_α and H_{II} phases in lipid–water phase dia-

grams. In a cubic phase structure the lipid monolayer curvature is balanced by the tendency of the molecules to adopt a wedge-like shape and the packing constraints of the hydrocarbon chains in the midplane of the bilayer (Lindblom & Rilfors, 1989). DPG consequently has larger tendencies to form nonlamellar phases than DOPS and DOPG, which form just an L_α phase between 10 and 98 wt % water and up to at least 55 °C. This conclusion is reasonable since DOPG and DOPS have bulkier head-groups than DPG.

PS has been shown to form an H_{II} phase in the anhydrous state (Williams & Chapman, 1970; Hauser et al., 1982), and at low pH values, and in the presence of Li^+, at high water contents (see the introduction). PG seems to have no tendencies to form nonlamellar phases; it forms a lamellar phase even in the presence of divalent cations (Farren & Cullis, 1980). With the knowledge now existing for the four anionic phospholipids that have been studied in this work, they can be graded in the following way with respect to their ability to form nonlamellar phases: PA > DPG > PS > PG. The phase behavior of DOPA and DPG shows that it cannot be assumed per se that phospholipids having charged head-groups only form an L_α phase together with pure water.

It is well documented that the addition of anionic phospholipids to an H_{II} phase formed by PE or monoglucosyldiacylglycerol (MGlcDG) breaks up this phase and converts it to an L_α phase [see Rilfors et al. (1984)]. In this investigation, DOPG was added to an H_{II} phase formed by DOPC–*n*-dodecane–water, but the H_{II} phase persisted; an H_{II} phase was obtained even by a DOPG–*n*-dodecane–water mixture. Thus, the packing constraints of the hydrocarbon chains, which opposes the formation of nonlamellar phases, is removed by the presence of the alkane (Gruner, 1985; Sjölund et al., 1987, 1989), and even a lipid like PG then forms an H_{II} phase.

Water Quadrupole Splittings. ^2H and ^{23}Na NMR quadrupole splittings were obtained at high water contents from all four lipid–water systems (Figures 5–7). The decrease in the water ^2H quadrupole splitting with increasing water content can be rationalized by applying a two-site model (Finer & Darke, 1974; Arvidson et al., 1985) where "free" and "bound" water molecules are assumed to exchange rapidly between the sites. The observed quadrupole splitting within this model then follows

$$\Delta^2H = nX_L/X_W|\chi S| \quad (1)$$

where X_L and X_W are the mole fractions of lipid and water, χ is the quadrupole coupling constant, n is the average number of water molecules bound to each head-group, and S is the order parameter describing an average orientational order of the water molecules.

The observed quadrupole splittings follow eq 1 and give a straight line, passing through the origin, over the whole range of water concentrations studied for DOPA (Figure 6) and DOPG. A behavior according to eq 1 is not obtained for DOPS and DPG at low water contents, but it is approximately followed at high water concentrations. The slope of the straight lines obtained are given in Table I together with the ^{23}Na quadrupole splittings at high water concentrations, where these have reached a constant value for each of the lipid systems. The slope, $n(\chi S)$, decreases in the order DOPA $\approx$ DPG > DOPS > DOPG. The value of the ^{23}Na quadrupole splittings follow the same trend and exhibit a similar relative change as the ^2H quadrupole splittings, indicating that the changes in the ^2H and ^{23}Na NMR data observed for the different lipid–water systems are caused by a common factor. The change in the slopes shown in Table I can be due to either a change in the hydration of the head-group, n, or a change in the order parameter, S, since χ is intramolecular and a constant equal to about 220 kHz (Glasel, 1972). The fraction of counterions associated to the charged bilayers is very high, and there is nearly a complete coverage of the negative head-groups (see below). If the assumption is made that the sodium–phosphate interaction is similar for the different lipids, i.e., the quadrupole coupling constant of the sodium nuclei is the same for all the lipid systems, this leads to the conclusion that the difference in the ^{23}Na splittings of the various lipid systems is due to a change in the order parameter, S (cf. eq 3 below). It seems very probable that the quadrupole splitting of the water molecules is affected by the same, or a similar, ordering mechanism in the polar head-group region and thus follows a similar trend. Therefore, the experimental findings in Table I strongly indicate that the molecular order in the head-group region of the lipid bilayers decreases in the order DOPA $\approx$ DPG > DOPS > DOPG, i.e., in a similar way as the ability of these lipids to form nonlamellar phase structures (see above). This conclusion seems very reasonable considering the fact that the polar head-groups of DOPA and DPG are smaller than those of DOPS and DOPG. The bulkier head-groups of the latter two lipids most probably create more disorder in the head-group region, leading to a smaller order parameter for both the water molecules and the sodium ions. Consequently, a decrease will be observed in the quadrupole splitting for both these species.

From the deuterium quadrupole splittings of ^2H_2O in the DOPA–water and DOPG–water systems (cf. Figure 6), it can be concluded that the bilayers in the L_α phase are fully hydrated already at rather low water contents and that further addition of water only results in an increase of "free" water molecules between the lamellae. It is interesting to note that the nonionic sugar lipids MGlcDG and diglucosyldiacylglycerol (DGlcDG) have a comparatively much lower ability to take up water, whether the phase is lamellar (DGlcDG) or reversed hexagonal (MGlcDG) (Lindblom et al., 1986). The main reason for this is that there are no large repulsive forces due to long-range Columbic interactions. Furthermore, short-range repulsive forces are also much weaker for the nonionic glucolipids than for the phospholipids (Marra, 1986; Lindblom et al., 1986). A recent publication by Israelachvili and Wennerström (1990) gives a possible explanation to this behavior. They discuss the effect of steric forces between amphiphilic surfaces, and, most probably, the steric or protrusion force between the glucolipid aggregates is diminished by the decreased mobility of the sugar head-groups due to hydrogen bonding (A. Holmgren, L. Rilfors, and G. Lindblom, to be published).

Sodium Ion Binding. The experimental discovery, 20 years ago, of quadrupole splittings of sodium counterions in lyotropic liquid-crystalline systems (Lindblom, 1971) has made it possible to very conveniently study the degree of ion binding of quadrupolar nuclei, as for example ^{23}Na, in lamellar and hexagonal phases. It should be noted that this NMR method is probably still the only one with which ion binding in lyotropic liquid crystals can be directly investigated. A nonzero electric field gradient arises when the ion is close to a charged surface so that the solvation shell of the ion at an interface will be asymmetric (Wennerström et al., 1974). Previously it has been demonstrated that the ions close to the aggregate surface give a contribution to the observed quadrupole splitting, while those away from the surface show no splitting (Wennerström et al., 1974; Lindblom et al., 1976a,b, 1978; Tiddy et al., 1978). There is a fast chemical exchange between "free" and "bound" ions, hence the observed splitting (cf. the description of water

quadrupole splittings above) can be described as

$$\Delta^{23}\mathrm{Na} = p_f\Delta_f + p_b\Delta_b \quad (2)$$

where the subscripts f and b refer to free and bound ions. If there are several different bound sites, the observed splitting is the average over all the sites:

$$\Delta^{23}\mathrm{Na} = p_{bi}\Delta_{bi} \quad (3)$$

where it has been assumed that Δ_f is equal to zero. Figure 7 shows that at water concentrations between about 50 and 98 wt % the ^{23}Na quadrupole splitting is constant for all the anionic lipids studied, implying that the fraction of bound ions, p_b, is constant over a large range of water concentrations. This kind of ion binding has previously been observed for lamellar liquid crystals composed of simple amphiphiles like soaps and water (Wennerström et al., 1979, and references therein), and it was described by a so-called "ion condensation" model (Manning, 1972). In the ion condensation model, the counterions are assumed to bind to the charged surfaces of the lamellar aggregates to reduce the effective charge density to a constant critical value. For a brief description of the electrostatic properties of charged bilayers, see Appendix.

It can be concluded that almost all of the counterions are located close to the bilayer surfaces, balancing the surface charge (see Appendix). Furthermore, according to eq A4, the counterion concentration close to the bilayer surface will not depend on the water content between the bilayers at sufficiently large interbilayer distances (Wennerström et al., 1979). This is in accordance with the experimental observation for all the anionic lipids studied here at high water concentrations (Figure 7).

The counterion association to the aggregate surface is high also for the H_{II} phase (see Appendix). However, it is somewhat smaller than for the L_α phase, since the contact density of a cylinder is smaller than that of a plane with the same charge density and osmotic pressure (Wennerström et al., 1982).

It can be shown (Wennerström et al., 1974) that the value of the quadrupole splitting of a lamellar phase is twice that of a hexagonal phase, considering only the difference in geometry between the two phases, i.e., it is assumed that the interactions between the counterions and the aggregate surface (p_i, local order parameter, electric field gradient, number of sites, etc.) are the same in the lamellar and hexagonal phases. It was found for a two-phase sample of DOPA–water that the ^{23}Na quadrupole splitting was equal to 26.8 kHz for the L_α phase and 16.2 kHz for the H_{II} phase (Figure 5D). Thus, the ratio between the observed splittings for the two phases is sufficiently close to the theoretical value of 2, considering the number of assumptions involved. It has been observed previously for other liquid-crystalline systems, where ion condensation does *not* occur, that the quadrupole splittings in lamellar and hexagonal phases often are of comparable and much smaller magnitude [see, for example, Persson et al. (1974)]. The relatively large splitting obtained for the H_{II} phase is most probably due to a larger Δ_{bi} experienced by the sodium ions at the highly curved aggregate surfaces in this phase.

Note that the result of the ion condensation model is in sharp contrast to that expected from a simple chemical equilibrium model having a single type of binding site characterized by one binding constant. In such a model a dilution of the system would lead to a decrease in the number of bound ions, which would be reflected in a decrease in the measured ^{23}Na quadrupole splitting. A change in the splitting is observed at lower water contents for DPG, DOPS, and DOPG, where the ion condensation model no longer is applicable (Figure 7). It has previously been shown (Lindblom et al., 1975) that this behavior of the splitting arises from a change in the effective angle between the electric field gradient and the director, probably due to a change in p_{bi} at the different binding sites having an opposite sign of the order parameter S_i. This latter parameter characterizes the ordering of the ions in the different sites. A possible explanation could then be that at high water contents the sodium ions reside on the edge of the polar head-groups, causing the electric field gradient to be more or less perpendicular to the aggregate surface. When the water concentration is reduced, the counterions may replace the water molecules between the polar head-groups and the order parameters may change sign upon such a process, if the two sites in question are located on different sides of the "magic angle". Alternatively, there might be two different binding sites on the phosphate group, also having opposite signs of the order parameter. It should be noted that the quadrupole splitting of the water molecules, as well as the splitting from the ions, *increases* with increasing temperature. These experimental findings again support a model with several binding sites having order parameters of different signs.

Concluding Remarks

The phase behavior of the different anionic phospholipids in water was found to depend strongly on the chemical structure of the polar head-group. The formation of the various phase structures can be rationalized by simple theoretical models. The interplay between the steric repulsion of the lipid head-groups and the counterion association to the aggregate surfaces is found to be important for determining the differences in the phase behavior for these systems. Thus, the larger head-groups of DOPS and DOPG make these lipids form only L_α phases, while DOPA, having a comparatively small head-group when the electrostatic repulsive force is diminished by a high counterion association, may form nonlamellar structures. DPG exhibits a phase behavior that lies in between that of DOPA, on one hand, and DOPS or DOPG on the other hand. The observed quadrupole splittings of water and sodium counterions indicate that the molecular order in the polar head-group region decreases for the L_α phase in the order DOPA $\approx$ DPG > DOPS > DOPG. For all the anionic phospholipids studied, it was observed that at water contents above about 50 wt %, the fraction of counterions located close to the interfacial surface of the aggregate was constant, very high (>95%), and independent of the water concentration. Such a distribution of counterions at a charged colloid surface can be described by the simple Poisson–Boltzmann theory and is often called "ion condensation". Since the number of bound ions is unaffected by a dilution of the system, i.e., it is independent of the water content as long as the surface charge density is sufficiently large, such an ion condensation behavior may have interesting biological implications. For example, it should be an energetic advantage for the cell to have the appropriate ions, participating in a transmembrane or a lateral transport, located close to the cell surface. An ion condensation mechanism might be a suitable possibility, facilitating such a process.

Acknowledgments

We thank Sol Gruner, Paul Harper, Adrian Parsegian, and Dave Siegel for valuable comments on the manuscript.

Appendix

Let us briefly look into the counterion distribution between two similarly charged planar surfaces in pure water

(Wennerström et al., 1982). In this consideration the counterions are treated as point charges embedded in a dielectric continuum of relative permittivity ϵ, bounded by two planar negatively charged surfaces of surface charge density σ. In a mean-field approximation, the counterion concentration at a point x between the two surfaces is determined by the electrostatic potential ϕ, which is obtained by solving the Poisson–Boltzmann equation

$$\Delta\phi = -(zen_0/\epsilon\epsilon_0) \exp(-ze\phi/kT) \quad \text{(A1)}$$

where Δ is the Laplacian, z is the valency of the ions, n_0 is the concentration of ions at the midplane ($x = 0$) and the other symbols have their usual meaning. By using the appropriate boundary conditions for this planar system, it is found that the counterion concentration, n_x, at any point x is given by

$$n_x = n_0 + \epsilon\epsilon_0/2kT(d\phi/dx)_x^2 \quad \text{(A2)}$$

and, since $d\phi/dx$ at the surface is equal to $\sigma/\epsilon\epsilon_0$, the ion concentration at the planar surface is then given by

$$n_{surface} = n_0 + \sigma^2/2\epsilon\epsilon_0 kT \quad \text{(A3)}$$

Equation A3 is called the contact value theorem (Henderson & Blum, 1978, 1981; Henderson et al., 1979; Wennerström et al., 1982). It can be concluded from this equation that the counterion concentration at the surface is independent of the ion valency z and that, for two surfaces that are far apart, n_0 will approach zero, and we have

$$n_{surface} = \sigma^2/2\epsilon\epsilon_0 kT \quad \text{(A4)}$$

This relation can be used to calculate the counterion concentration at the surface of a charged bilayer. For the DOPA–water system at 298 K, setting $\sigma = -2e/a_0 = -0.5$ C·m^{-2} with $a_0 = 0.65$ nm^2 (Figure 3C), we get $n_{surface} = 4 \times 10^{28}$ ions·m^{-3}. Assuming that the ions are residing within 0.1 nm of the charged interface, then the above value for $n_{surface}$ corresponds to about 4 ions·nm^{-2}. This value is comparable with the surface charge density σ, which is equal to about three elementary charges per nm^2. A calculation leading to similar results can be made for all the other anionic lipids studied in this work.

The counterion distribution in H_{II} phases can be treated in the same way, setting out with solving the Poisson–Boltzmann equation for cylindrical geometry. An analytical solution of such a case was recently provided by Furo et al. (1990). Applying their eq B7 on the H_{II} phase of the DOPA–water system, the fraction of counterions in the interfacial region of cylinders having a radius of 25 Å (Figure 3B) can be calculated to be about 95%.

Supplementary Material Available

One figure showing the water quadrupole splitting as a function of the water concentration for the systems DOPG–water, DOPS–water, and DPG–water (1 page). Ordering information is given on any current masthead page.

Registry No. DOPA, 14268-17-8; DOPS, 6811-55-8; DOPG, 62700-69-0; NaCl, 7647-14-5; $Me(CH_2)_{10}Me$, 112-40-3; Na, 7440-23-5.

References

Antonenko, Y. N., & Yaguzhinsky, L. S. (1990) *Biochim. Biophys. Acta 1026*, 236.

Arvidson, G., Brentel, I., Khan, A., Lindblom, G., & Fontell, K. (1985) *Eur. J. Biochem. 152*, 753.

Brentel, I., Selstam, E., & Lindblom, G. (1985) *Biochim. Biophys. Acta 812*, 816.

Brentel, I., Arvidson, G., & Lindblom, G. (1987) *Biochim. Biophys. Acta 904*, 401.

Cevc, G., Seddon, J. M., & Marsh, D. (1985) *Biochim. Biophys. Acta 814*, 141.

Christiansson, A., Eriksson, L. E. G., Westman, J., Demel, R., & Wieslander, Å. (1985) *J. Biol. Chem. 260*, 3984.

Cullis, P. R., Verkleij, A. J., & Ververgaert, P. H. J. T. (1978) *Biochim. Biophys. Acta 513*, 11.

Davis, J. H., Jeffrey, K. R., Bloom, M., Valic, M. I., & Higgs, T. P. (1976) *Chem. Phys. Lett. 42*, 390.

De Kroon, A. I. P. M., Timmermans, J. W., Killian, J. A., & De Kruijff, B. (1990) *Chem. Phys. Lipids 54*, 33.

Demel, R. A., Paltauf, F., & Hauser, H. (1987) *Biochemistry 26*, 8659.

Eriksson, P.-O., Rilfors, L., Lindblom, G., & Arvidson, G. (1985) *Chem. Phys. Lipids 37*, 357.

Farren, S. B., & Cullis, P. R. (1980) *Biochem. Biophys. Res. Commun. 97*, 182.

Farren, S. B., Hope, M. J., & Cullis, P. R. (1983) *Biochem. Biophys. Res. Commun. 111*, 675.

Findlay, E. J., & Barton, P. G. (1978) *Biochemistry 17*, 2400.

Finer, E. G., & Darke, A. (1974) *Chem. Phys. Lipids 12*, 1.

Fontell, K., Mandell, L., Lehtinen, H., & Ekwall, P. (1968) *Acta Polytech. Scand., Chem. Technol. Metall. Ser. 74, III*, 1.

Furo, I., Halle, B., Quist, P.-O., & Wong, T. C. (1990) *J. Phys. Chem. 94*, 2600.

Girault, H. H. J., & Schiffrin, D. J. (1984) *J. Electroanal. Chem. 179*, 227.

Girault, H. H. J., & Schiffrin, D. J. (1986) *Biochim. Biophys. Acta 857*, 251.

Glasel, J. A. (1972) in *Water: A Comprehensive Treatise* (Franks, F., Ed.) Vol. 1, p 215, Plenum Press, New York.

Gruner, S. M. (1985) *Proc. Natl. Acad. Sci. U.S.A. 82*, 3665.

Gulik-Krzywicki, T., Tardieu, A., & Luzzati, V. (1969) *Mol. Cryst. Liq. Cryst. 8*, 285.

Haines, T. H. (1983) *Proc. Natl. Acad. Sci. U.S.A. 80*, 160.

Harlos, K., & Eibl, H. (1981) *Biochemistry 20*, 2888.

Hauser, H. (1984) *Biochim. Biophys. Acta 772*, 37.

Hauser, H. (1989) *Proc. Natl. Acad. Sci. U.S.A. 86*, 5351.

Hauser, H., Paltauf, F., & Shipley, G. G. (1982) *Biochemistry 21*, 1061.

Helfrich, W. (1973) *Z. Naturforsch. C 28*, 693.

Henderson, D., & Blum, L. (1978) *J. Chem. Phys. 69*, 5441.

Henderson, D., & Blum, L. (1981) *J. Chem. Phys. 75*, 2025.

Henderson, D., Blum, L., & Lebowitz, J. L. (1979) *J. Electroanal. Chem. Interfacial Electrochem. 102*, 315.

Hope, M. J., & Cullis, P. R. (1980) *Biochem. Biophys. Res. Commun. 92*, 846.

Hyde, S. T. (1989) *J. Phys. Chem. 93*, 1458.

Israelachvili, J. N., & Wennerström, H. (1990) *Langmuir 6*, 873.

Israelachvili, J. N., Marcelja, S., & Horn, R. G. (1980) *Q. Rev. Biophys. 12*, 121.

Jacobson, K., & Papahadjopoulos, D. (1975) *Biochemistry 14*, 152.

Kaminoh, Y., Kano, F., Chiou, J.-S., Kamaya, H., Lin, S. H., & Ueda, I. (1988) *Biochim. Biophys. Acta 943*, 522.

Kanemasa, Y., Yoshioka, T., & Hayashi, H. (1972) *Biochim. Biophys. Acta 280*, 444.

Kirk, G. L., & Gruner, S. M. (1985) *J. Physique 46*, 761.

Kogut, M., & Russell, N. J. (1984) *Curr. Microbiol. 10*, 95.

Komaratat, P., & Kates, M. (1975) *Biochim. Biophys. Acta 398*, 464.

Lindblom, G. (1971) *Acta Chem. Scand. 25*, 2767.

Lindblom, G. (1972) *Acta Chem. Scand. 26*, 1745.
Lindblom, G., & Rilfors, L. (1989) *Biochim. Biophys. Acta 988*, 221.
Lindblom, G., & Rilfors, L. (1990) *Dynamics and Biogenesis of Membranes* (Op den Kamp, J. A. F., Ed.) NATO ASI Series Vol. H 40, p 43, Springer Verlag, Berlin.
Lindblom, G., Tiddy, G. J. T., & Lindman, B. (1975) *Acta Chem. Scand., Ser. A 29*, 876.
Lindblom, G., Persson, N.-O., & Arvidson, G. (1976a) *Adv. Chem. Ser. 152*, 121.
Lindblom, G., Wennerström, H., & Lindman, B. (1976b) *ACS Symp. Ser. 34*, 372.
Lindblom, G., Lindman, B., & Tiddy, G. J. T. (1978) *J. Am. Chem. Soc. 100*, 2299.
Lindblom, G., Brentel, I., Sjölund, M., Wikander, J., & Wieslander, Å. (1986) *Biochemistry 25*, 7502.
Lindblom, G., Sjölund, M., & Rilfors, L. (1988) *Liq. Cryst. 3*, 783.
Manning, G. S. (1972) *Annu. Rev. Phys. Chem. 23*, 117.
Marra, J. (1986) *J. Colloid Interface Sci. 109*, 11.
McLaughlin, A. C., Cullis, P. R., Berden, J. A., & Richards, R. E. (1975) *J. Magn. Reson. 20*, 146.
Miller, K. J. (1985) *J. Bacteriol. 162*, 263.
Mombers, C., Van Dijck, P. W. M., Van Deenen, L. L. M., De Gier, J., & Verkleij, A. J. (1977) *Biochim. Biophys. Acta 470*, 152.
Ohno, Y., Yano, I., & Masui, T. (1979) *J. Biochem. (Tokyo) 85*, 413.
Op den Kamp, J. A. F., Redai, I., & Van Deenen, L. L. M. (1969) *J. Bacteriol. 99*, 298.
Papahadjopoulos, D., Vail, W. J., Newton, C., Nir, S., Jacobson, K., Poste, G., & Lazo, R. (1977) *Biochim. Biophys. Acta 465*, 579.
Persson, N.-O., Lindblom, G., Lindman, B., & Arvidson, G. (1974) *Chem. Phys. Lipids 12*, 261.
Rance, M., & Byrd, R. A. (1983) *J. Magn. Reson. 52*, 221.
Rand, R. P., & Sengupta, S. (1972) *Biochim. Biophys. Acta 255*, 484.
Reusch, R. N. (1990) *Chem. Phys. Lipids 54*, 221.
Rilfors, L., Lindblom, G., Wieslander, Å., & Christiansson, A. (1984) *Biomembranes 12*, 205.
Rilfors, L., Eriksson, P.-O., Arvidson, G., & Lindblom, G. (1986) *Biochemistry 25*, 7702.
Rosevear, F. B. (1954) *J. Am. Oil Chem. Soc. 31*, 628.
Rosevear, F. B. (1968) *J. Soc. Cosmet. Chem. 19*, 581.
Seddon, J. M., Kaye, R. D., & Marsh, D. (1983) *Biochim. Biophys. Acta 734*, 347.
Sjölund, M., Lindblom, G., Rilfors, L., & Arvidson, G. (1987) *Biophys. J. 52*, 145.
Sjölund, M., Rilfors, L., & Lindblom, G. (1989) *Biochemistry 28*, 1323.
Tate, M. W., & Gruner, S. M. (1987) *Biochemistry 26*, 231.
Tate, M. W., Eikenberry, E. F., Turner, D. C., Shyamsunder, E., & Gruner, S. M. (1991) *Chem. Phys. Lipids 57*, 147.
Tiddy, G. J. T., Lindblom, G., & Lindman, B. (1978) *J. Chem. Soc., Faraday Trans. 1 74*, 1290.
Tilcock, C. P. S., & Cullis, P. R. (1982) *Biochim. Biophys. Acta 684*, 212.
Ulmius, J., Wennerström, H., Lindblom, G., & Arvidson, G. (1977) *Biochemistry 16*, 5742.
Van Dijck, P. W. M., De Kruijff, B., Verkleij, A. J., Van Deenen, L. L. M., & De Gier, J. (1978) *Biochim. Biophys. Acta 512*, 84.
Van Venetië, R., & Verkleij, A. J. (1981) *Biochim. Biophys. Acta 645*, 262.
Wennerström, H., Lindblom, G., & Lindman, B. (1974) *Chem. Scr. 6*, 97.
Wennerström, H., Lindman, B., Lindblom, G., & Tiddy, G. J. T. (1979) *J. Chem. Soc., Faraday Trans. 1 75*, 663.
Wennerström, H., Jönsson, B., & Linse, P. (1982) *J. Chem. Phys. 76*, 4665.
Verkleij, A. J., De Kruijff, B., Ververgaert, P. H. J. T., Tocanne, J. F., & Van Deenen, L. L. M. (1974) *Biochim. Biophys. Acta 339*, 432.
Verkleij, A. J., De Maagd, R., Leunissen-Bijvelt, J., & De Kruijff, B. (1982) *Biochim. Biophys. Acta 684*, 255.
Williams, R. M., & Chapman, D. (1970) *Prog. Chem. Fats Lipids 11*, 1.